

Helium Emissions Observed in Ground-Based Spectra of Solar Prominences

R. Ramelli¹ · G. Stellmacher² · E. Wiehr³ · M. Bianda¹

© Springer ●●●●

Abstract

The only prominent line of singly ionized helium in the visible spectral range, He II 4686Å, is observed together with the He I 5015Å singlet and the He I 4471Å triplet line in solar prominences. The Na D₂ emission is used as a tracer for He II emissions which are sufficiently bright to exceed the noise level near 10⁻⁶ of the disk-center intensity. The so selected prominences are characterized by small non-thermal line broadening and almost absent velocity shifts, yielding narrow line profiles without wiggles. The reduced widths [$\Delta\lambda_D/\lambda$] of He II 4686Å are 1.5 times broader than those of He I 4471Å triplet and 1.65 times broader than those of He I 5015Å singlet. This indicates that the He lines originate in a prominence–corona transition region with outwards increasing temperature.

Keywords: Prominences, Quiescent, Helium ionization

1. Introduction

As the second most abundant element, helium plays an essential role in astrophysics. Nevertheless, its spectrum is poorly understood. The faint He II 4685.7Å line is of particular interest, since it is the only important He II line that can be observed with ground-based telescopes allowing higher spectral resolution than currently achieved for EUV He II lines from space: Stellmacher, Wiehr, and Dammasch (2003) find that the SUMER spectrograph (designed for broad coronal lines) does not resolve the narrow emissions from cool prominences, even after application of a maximum instrumental profile.

He II 4685.7Å has been observed in prominences during eclipses (Sotirovski, 1965; Poletto, 1967). Line-profile analyses, based on moderately resolved spectra from coronagraphs (Hirayama, 1972; Hirayama and Nakagomi, 1974) indicate that He II 4685.7Å originates from the same (cool) prominence regions as the usually observed Balmer, He I and metallic lines. Tandberg-Hanssen and Zirin (1959)

¹ Istituto Ricerche Solari, Locarno, Switzerland, email: ramelli@irsol.ch and mbianda@irsol.ch

² Institute d'Astrophysique, Paris, France, email: stell@iap.fr

³ Institut für Astrophysik, Göttingen, Germany, email: ewiehr@astro.physik.uni-goettingen.de

observe in "flare-like loop" (*i.e.* highly active and "hot") prominences the width of He II 4685.7Å larger than that of He I 4471.5Å, however, they neither discuss quiescent ("cool") prominences nor the atomic fine-structure broadening of He II which may explain most of that excess. A detailed analysis of the He I and He II lines in solar prominences requires high spectral resolution, high signal-to-noise ratio and careful absolute calibration, which is difficult to achieve (see Illing, Landman, and Mickey, 1975), but is possible with modern CCD techniques.

The high ionization and excitation energy of 25 and 48 eV suggests that He II 4685.7Å may preferentially occur in hot prominences ($T_{\text{kin}} > 8000\text{K}$) which are observed to have a high He-to-Balmer emission ratio and to be highly structured (Stellmacher and Wiehr, 1994). These, however, usually show important velocity shifts which disperse the line profiles. We therefore suppose that the chance to measure He II 4685.7Å increases *if the emitted photons are concentrated in wavelength, i.e. yield narrow line profiles free from spatial Doppler shifts*. Such emissions should occur in prominences with negligible macro-velocities and low non-thermal line broadening, which are known to be bright in H α though with a low He-to-Balmer ratio (Engvold and Livingston, 1971; Stellmacher and Wiehr, 1995). Such prominences show significant Na D and Mg b emission and saturated H α (and even H β) profiles but did so far not allow a He II 4685.7Å line profile analysis (Stellmacher and Wiehr, 2005).

2. Observations

In August 2011 we observed prominence emissions with the Gregory-Coudé telescope at the Locarno Solar Observatory (IRSOL: Ramelli *et al.*, 2006). The faint He II 4685.7Å emission is hardly visible in the raw spectra and can only be detected after careful subtraction of the superposed aureole spectrum. We therefore used the Na D₂ emission as a visual tracer for prominence candidates with "spectral photon concentration" and thus sufficient He II radiance. The so selected emission regions elevated only few arc-seconds over the limb and occurred at low solar latitudes $\varphi < 30^\circ$. We oriented the spectrograph slit perpendicular to the solar limb by means of an image rotator, and pointed the telescope so that the light of the solar disk did not pass the aperture in the prime focus (*cf.*, slit-jaw images in Figure 1). This avoids an illumination of the secondary and the two folding flat mirrors of the telescope thus reducing the stray-light (*cf.*, Figure 2 in Stellmacher and Wiehr, 1970) - in our case by almost a factor of two.

In order to obtain a sufficiently high signal-to-noise ratio for the faint He II line, we chose a slit width of two arc-seconds and superposed spectra of (typically) 10 seconds exposure, yielding total integration times between 50 and 300 seconds. We used an unmasked "e2v CCD 55-30" sensor mounted on a ZIMPOL camera (Ramelli *et al.*, 2010) and operated the ZIMPOL system only in its intensity mode (Stokes *I*). The flat-field was deduced from attenuated disk-center spectra which also served for the absolute calibration of the emissions. We took these spectra under identical conditions (exposure, slit width) as those for the prominence (and aureole) except for a defined attenuation of the high disk-center

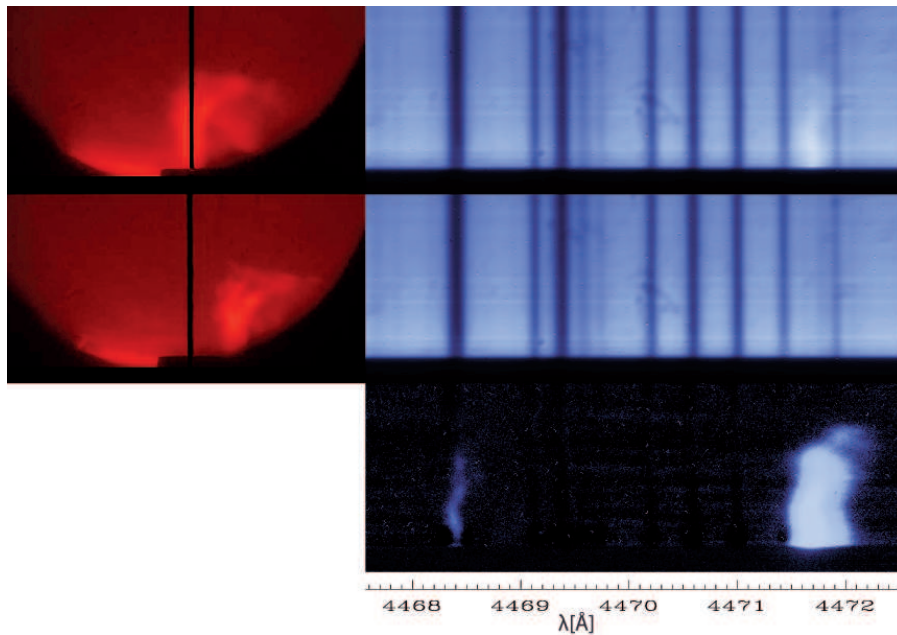


Figure 1. Raw spectra of a prominence (upper right panel) and the neighboring aureole (middle panel), i.e. the prominence displaced by a few arc-seconds from the slit (see left panels); difference image (lower panel) with prominence emissions, color scale adapted to the faint Ti II 4468.4Å, the strong He I 4471.5Å emission thus over-saturated; the H α slit jaw images show the chromosphere just at their bottoms, the solar disk is outside the field-stop in the primary focus, seen as round image boundary in the left panels.

light level using carefully calibrated neutral filters. This allows to express the CCD counts of the prominence emission in terms of CCD counts at disk-center which finally are converted into absolute radiance [$\text{erg s}^{-1} \text{cm}^{-2} \text{sterad}^{-1}$] using the tables of Labs and Neckel (1970).

The prominence emissions are superposed by an absorption spectrum from the solar disk (the "aureole") which is due to Rayleigh scattering mostly by dust particles on the telescope mirrors and less in Earth's atmosphere (*cf.*, Figure 2 in Stellmacher and Wiehr, 1970); it decreases in brightness with distance from the limb. We took such aureole spectra in the immediate vicinity of the respective prominence, normalized them to fit the spatial intensity distribution of the prominence spectra outside their emission lines, and subtracted them from the prominence spectral images (see Figure 1). The "zero level" of the resulting emission spectra is disturbed by spurious remnants of the aureole lines arising from small (sub-pixel) spectral shifts between prominence and aureole exposure (spectrograph seeing). That " λ -offset" produces signatures that are anti-symmetrically shaped and can be described by the derivative of the aureole absorption profiles. We largely remove these signals by either adding or subtracting a fraction of the derivative of the respective aureole spectral profile. In the corrected spectra we finally select spatial prominence regions with strong emission and negligible Doppler structures.

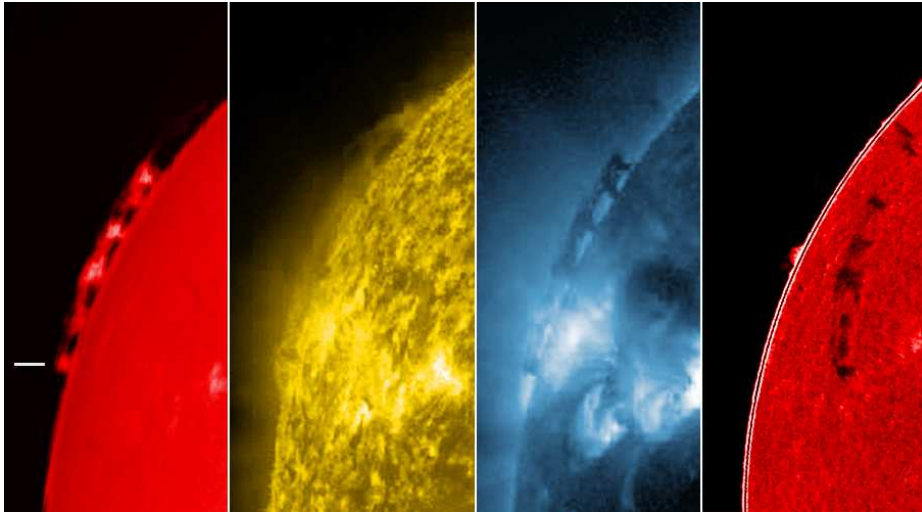


Figure 2. Images of the prominence chain at the east limb $+10^\circ < \psi < +35^\circ$ on August 4, 2011, in $H\alpha$ from the Kanzelhöhe Observatory (left panel, the observed prominence at 14° N marked), in $\text{He II } 304\text{\AA}$ and $\text{Fe XVI } 335\text{\AA}$ from SDO/AIA (middle panels), together with the corresponding disk filament on August 6 (right panel, Kanzelhöhe).

On 2 and 4 August we observed exclusively Na D_2 , $\text{He II } 4685.7\text{\AA}$ and the $\text{He I } 4471.5\text{\AA}$ triplet line. After preliminary data reduction, we decided to include the $\text{He I } 5015.7\text{\AA}$ singlet line as well. The first spectrum of that line (August 9) showed the emission of the neighboring $\text{Fe II } 5018.4$ line, drawing our attention also to the faint $\text{Ti II } 4468.4\text{\AA}$ line in the vicinity of $\text{He I } 4471.5\text{\AA}$. The occurrence of such "chromospheric emissions", usually observed only during solar eclipses, establishes our selection criterion and demonstrates the high quality of our observations. On August 13 we added further metallic lines with significant emission in the table of Sotirovski (1965).

Among dozens of prominences occurring in the first half of August 2011, we found only few with markedly bright and narrow Na D_2 profiles, however, only four of these showed measurable $\text{He II } 4685.7\text{\AA}$ emission. The range of observed total $\text{He I } 4771.5\text{\AA}$ emission (radiance) $745 < E(4471) < 5120$ (see Table 1), largely exceeds the values $E(4471) < 320$ [$\text{erg s}^{-1} \text{cm}^{-2} \text{sterad}^{-1}$] by Stellmacher and Wiehr (1997). This shows that prominences with high He I radiance also yield a sufficient He II emission above the noise level of few 10^{-6} of the disk-center brightness (see Figure 3). Indeed, the chain of neighboring prominences occurring on August 4 at the east limb between 10°N and 35°N contained two with directly visible Na D_2 emission, but only one (14°N , marked in Fig. 2) with Na D profiles narrow and bright enough to allow an observable $\text{He II } 4686$ emission. Neither the $H\alpha$ or the $\text{He II } 304\text{\AA}$ appearance above the limb nor that of the corresponding filament on the disk and even not the cold prominence body, seen in the $\text{Fe XVI } 335\text{\AA}$ image as Lyman and He I continuum absorption, give an indication for a peculiarity of that prominence (E, 14°N) favoring the detectability of a $\text{He II } 4685.7\text{\AA}$ emission.

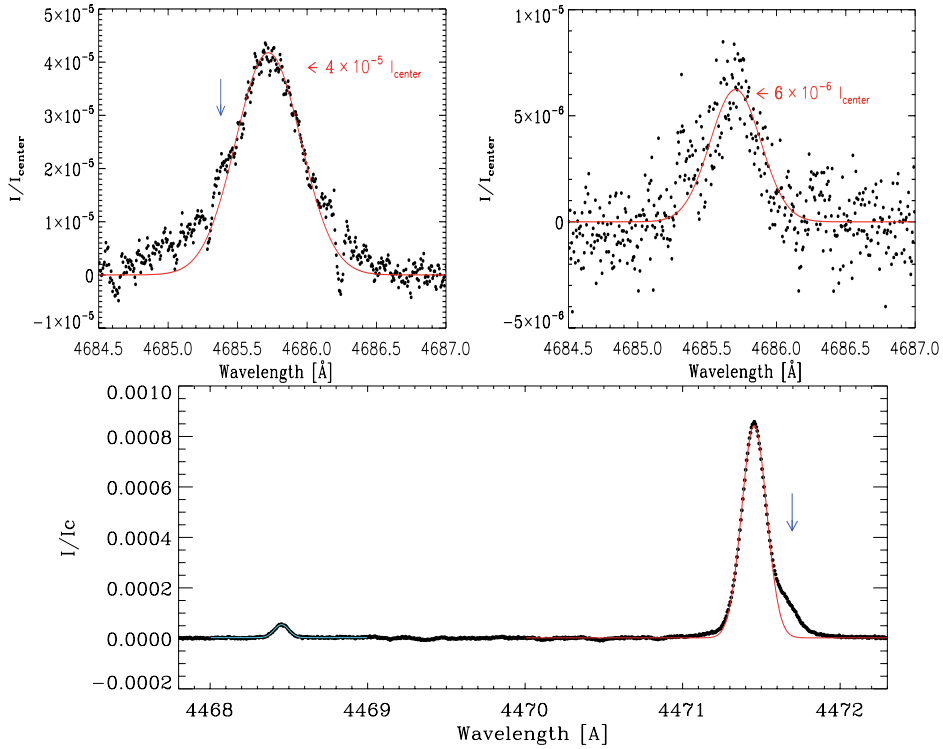


Figure 3. Strongest and faintest He II 4685.7 Å profiles from 2 and 13 August (note the different ordinate scales) together with Ti II 4468.4 Å and He I 4471.5 Å (*cf.*, lower panel of Fig 1). The colored lines give Gaussian fits to the upper profile parts. The atomic fine-structure components at 4685.35 Å and at 4471.7 Å (blue arrows) prove the high spectral resolution achieved.

3. Results

3.1. Line Radiance

Figure 3 shows the strongest and the faintest He II emissions obtained at a noise level of $\pm 1 \cdot 10^{-6}$ of the disk-center radiance. In Table 1 we summarize the observed total line emission and compare them with observations by Sotirovski (1965) and by Poletto (1967). Our low-latitude prominences ($\varphi < 30^\circ$) show much stronger radiance of the helium lines than the eclipse observations. The highest observed Na D₂ radiance of 1010 [$\text{erg s}^{-1} \text{cm}^{-2} \text{sterad}^{-1}$] (see Table 1) corresponds to a total H α emission of 2.5×10^5 [$\text{erg s}^{-1} \text{cm}^{-2} \text{sterad}^{-1}$] which, in turn, is related to a large optical thickness of $\tau_0(\text{H}\alpha) \approx 7.0$ (according to observations by Stellmacher and Wiehr, 1994, 2005); this proves that our criterion indeed selects thick prominences.

We find mean radiance ratios $E(4471)/E(5015) = 8.7$ for triplet-to-singlet and $E(4471)/E(4686) = 51$ for triplet-to-He II (*cf.*, Table 1). These ratio values are comparable to those obtained by Sotirovski (1965) and by Poletto (1967) from eclipse observations, although our prominences are much brighter. Hence, the radiance ratios seem to be valid over a large range of He emission.

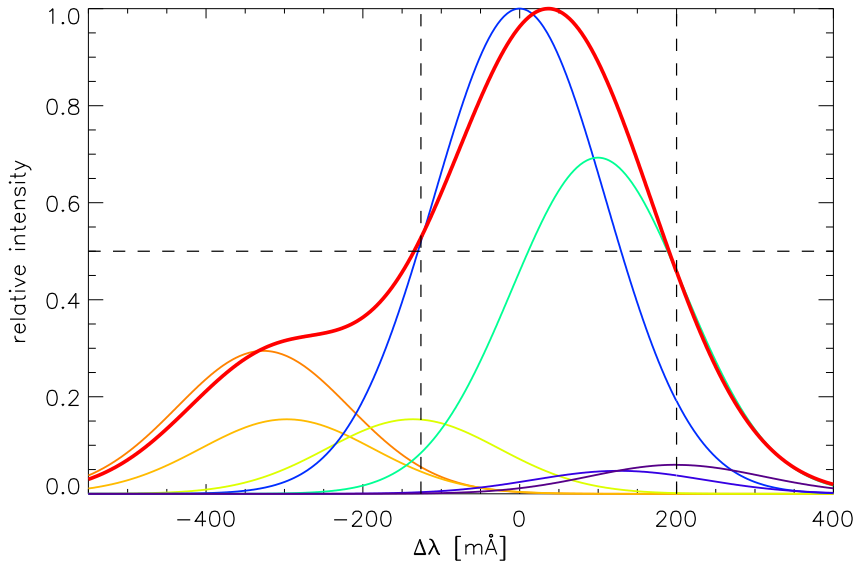


Figure 4. Superposition of the seven strongest (among 13) atomic fine-structure components of He II 4685.7, each one with FWHM=260 mÅ (chosen to fit the August 2 observation Figure 3). The resulting convoluted profile (red line, max. normalized) with FWHM=325 mÅ (dashed lines) is 1.25 times broader than the 'intrinsic' (*e.g.* blue) profile of each component.

3.2. Line Widths

The spectrograph slit of 0.25 mm width (corresponding to 2 arc-seconds) yields a typical instrumental line broadening of $\Delta\lambda_e/\lambda \approx 8 \times 10^{-6}$ which we apply to our observed line profiles. In addition, one has to consider the atomic fine-structure broadening: For He I 4471.5 five main components almost coincide ($\Delta\lambda = 19\text{mÅ}$); an additional faint component 210 mÅ red-wards (well visible in the lower panel of Figure 3) does not broaden the half-width, FWHM, of the composed profile.

He II 4685.7Å is composed of 13 atomic fine-structure components leading to a significant line broadening. A corresponding deconvolution has to take into account that the various atomic fine-structure components have different intensity but a unique ("intrinsic") width. He II 4685.7Å consists of two close main components ($\Delta\lambda = 0.53\text{mÅ}$, blue line in Fig. 4); a third one 100 mÅ red-wards (green line in Figure 4) broadens the FWHM of the composed profile (red line in Figure 4) by a factor of 1.25 which is independent from the intrinsic profile width. Two atomic fine-structure components (orange and yellow lines in Figure 4) produce a satellite at -350 mÅ which is hardly visible in the upper left panel of Figure 3 but does not influence the FWHM of the Gaussian fit to the upper part of the observed emission profile.

Considering the He II fine-structure broadening, we find that *the He II 4685.7Å line is 1.5 times broader than the He I 4471.5Å triplet line which, in turn, is 1.1 times broader than the He I 5015.7Å singlet line* (Table 2).

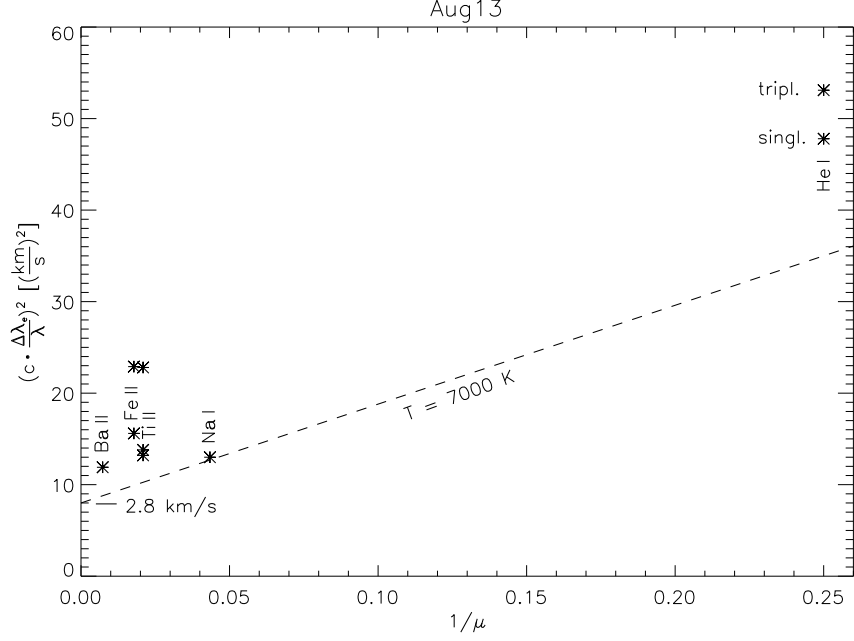


Figure 5. Velocity $v_o^2 = (c \cdot \Delta\lambda_D/\lambda)^2$ versus inverse atomic weight $1/\mu$ for the August 13 prominence; the dashed line connects $v_o^2(\text{Na I})$ with a reasonable $v_o^2(\text{H I})$ corresponding to $[\Delta\lambda_e/\lambda]_H = 3.7 \times 10^{-5}$ from Stellmacher and Wiehr (1994); the v_o^2 values of He II and of singly ionized metallic lines are located above that line; $v_o^2(\text{He II})=173$ is outside the ordinate range.

3.3. Kinetic Temperature

The Doppler widths $[\Delta\lambda_D]$ from atoms of different weight generally allows one to separate the thermal $[T_{\text{kin}}]$ from the (Maxwellian) non-thermal (v_{nth}) line broadening: $v_o^2 = (c \cdot \Delta\lambda_D/\lambda)^2 = 2RT_{\text{kin}}/\mu + v_{\text{nth}}^2$, if the lines are emitted in the same formation region. Associating $[v_o^2(1/\mu)]_{\text{Na D}}$ with $[v_o^2(1/\mu)]_{\text{He}}$ from the smallest He I (i.e. the singlet) line, we would obtain $T_{\text{kin}} \approx 10^4\text{K}$, a temperature too high for our selected dense, H α bright and optically thick prominences. These typically show for hydrogen $[\Delta\lambda_D/\lambda]_H = 3.7 \cdot 10^{-5}$ (Stellmacher and Wiehr, 1994) which would yield $T_{\text{kin}} = 7000\text{K}$ with the v_o value observed for Na D₂ on August 13 (dashed line in Figure 5). The corresponding ordinate offset gives a small value $v_{\text{nth}} = 2.8\text{ km/s}$ confirming our criterion of 'spectral photon concentration' (see introduction).

The v_o^2 values of the singly ionized metallic lines are found above the dashed line in Figure 5 indicating an excess broadening. This result disagrees with Landman (1985) who found Fe II 5169 smaller than Mg I b2 and b4. Also our observed v_o^2 values for He I singlet, triplet and He II are above the dashed line [$T_{\text{kin}} = 7000\text{K}$; $v_{\text{nth}} = 2.8\text{ km/s}$] in Figure 5. Keeping $v_{\text{nth}} = 2.8\text{ km/s}$, the widths of these three helium lines observed on August 13 would correspond to T_{kin} values of 9400 K, 10800 K and 40000 K, respectively; for constant $T_{\text{kin}} = 7000\text{K}$ they would yield v_{nth} values of 7.3, 8.1, and 15 km/s.

Table 1. Total line emission (radiance) [$\text{erg s}^{-1} \text{cm}^{-2} \text{sterad}^{-1}$] in comparison with eclipse data from Sotirovski (1965) and from Poletto (1967).

position obs.date	W22°N 2 Aug.	E14°N 4 Aug.	E30°N 9 Aug. a	E31°N 9 Aug. b	E23°N 13 Aug.	Soti- rovski	Poletto + Rigutti
He II 4685.7	105	35	38	–	13	4.0	5.5
He I 4471.5 (tr)	5119	1440	1940	1300	745	105	80
He I 5015.7 (si)	–	–	198	180	82	19	–
Fe II 5018.4	–	–	225	340	37	–	–
Ti II 4468.4	85	185	64	105	31	–	–
Na D ₂ 5890	1010	540	715	970	70	–	–
tripl/He II	49	41	50	–	63	26	15
tripl/singl	–	–	9.8	7.2	9.1	5.7	–
tripl/Na D ₂	3.0	2.7	2.7	1.3	10.6	–	–

4. Discussion

4.1. Line Radiance

In order to correctly describe the helium spectrum in the prominence plasma, one has to consider the statistical equilibrium of ortho-, para- and ionized helium and their interaction (*e.g.* Labrosse *et al.*, 2010). Observations of spectrally well resolved line profiles are required for the understanding of the helium spectrum. The optically thin He II 4685.7Å line is poorly documented from observations. Its excitation is sensitive to radiation and collisions (Yakovkin and Zeldina, 1971; Labrosse *et al.*, 2010), but also the influence of turbulence and of flows may enhance the He II emission (Jordan *et al.*, 1997; Patsourakos and Vial, 2002). A blending with Ni I 4686.22Å, mentioned by Worden, Beckers, and Hirayama (1973) in their study of chromospheric emissions, is not indicated in our prominence observations.

Our radiance ratio $7.2 < E(4471)/E(5015) < 9.8$ (Table 1) is in good agreement with $E(4471)/E(5015) = 9.5$ from models with $T = 8000 \text{ K}$ and $n_{\text{H}} \approx 10^{10} \text{ cm}^{-3}$ by Heasley, Mihalas, and Poland (1974). However, the radiance ratio $41 < E(4471)/E(4686) < 62$ found in our study as well as in the eclipse data (Sotirovski, 1965; Poletto, 1967) is smaller than $E(4471)/E(4686) = 6950$ obtained from those models. The latter ratio would predict for our faintest prominence (August 13 with $E(4471) = 745$) a He II 4685.7Å radiance of $E(4686) \approx 0.1$ [$\text{erg s}^{-1} \text{cm}^{-2} \text{sterad}^{-1}$] far below the noise level - even for eclipse observations. Those models are isothermal; recent models, however, with prominence–corona transition region, PCTR, show an increased He ionization (Labrosse and Gouttebroze (2004)). Our observed $E(4471)/E(4686)$ ratio is then in favor of an origin of He II 4685.7Å in the PCTR.

Table 2. Reduced Doppler widths $\Delta\lambda_D/\lambda$ [10^{-5}]; the values for He II 4685.7Å after deconvolution of the atomic fine-structure; numbers in parentheses give uncertainties originating from the fitting procedure.

emission line	2 Aug.	4 Aug.	9 Aug. a	9 Aug. b	13 Aug.
He II 4685.7	5.64 (0.12)	3.72 (0.13)	4.21 (0.22)	–	4.39 (0.39)
He I 4471.5 (tripl)	4.07 (0.01)	3.14 (0.02)	2.45 (0.01)	2.21 (0.01)	2.43 (0.01)
He I 5015.7 (singl)	–	–	2.24 (0.03)	2.07 (0.04)	2.28 (0.02)
Fe II 5018.4	–	–	1.53 (0.02)	1.05 (0.01)	1.32 (0.02)
Ti II 4468.4	3.28 (0.04)	2.30 (0.04)	1.17 (0.05)	0.92 (0.02)	1.21 (0.08)
Na D ₂ 5890	3.17 (0.60)	2.13 (0.03)	1.36 (0.02)	1.08 (0.01)	1.20 (0.01)
He II/tripl	1.37	1.18	1.72	–	1.80
tripl/singl	–	–	1.09	1.07	1.07
tripl/Na D ₂	1.30	1.47	1.79	2.05	2.13

4.2. Line Widths

A further hint of the PCTR contribution to the He lines is given by the different line widths observed for the three atomic states: singly ionized, triplet, singlet. The reduced width [$RW = \Delta\lambda_D/\lambda$] of the He II 4685.7Å line (after deconvolution of the atomic fine-structure) is significantly larger than that of the He I triplet line: $1.18 < RW(4686)/RW(4471) < 1.8$, and the triplet is broader than the singlet line: $1.07 < RW(4471)/RW(5015) < 1.09$ (see Table 2). The latter result disagrees with observations by Heasley, Tandberg-Hanssen, and Wagner (1975), bearing in mind their lower spectral resolution. Since the He I lines are even visible in our raw spectra (see Fig. 1; in contrast to the faint He II 4685.7Å), the observed excess width $RW(4471) > RW(5015)$ is outside the error bars of at most 2% (see Table 2).

The different widths of the He II, He I triplet and singlet lines may be due to their formation in prominence regions of different temperature. Indeed, Stellmacher, Wiehr, and Dammasch (2003) observe "hotter" lines to be more pronounced in such prominence regions which show less radiance in "cooler" lines. Labrosse (private communication, 2011) finds among 100 models with a PCTR of 10^5 K (*cf.*, Labrosse and Gouttebroze, 2004) mean ratios of the reduced widths of $1.1 < RW(4686)/RW(4471) < 1.6$ and $1.03 < RW(4471)/RW(5015) < 1.2$, respectively, in good agreement with our results. The PCTR then seems to be essential for an explanation of the the observed "hierarchy" of He line widths.

The difference between the singlet and the triplet emission is explained by the fact that the lowest He I energy level belongs to the singlet system which can thus be populated directly by EUV radiation, while the triplet levels are populated from the (singlet) ground state mainly by ionization and recombination. Collisional excitation plays a minor role in cool prominence regions, which are well visible as dark absorption features in the Fe XVI 335Å image (see Figure 2).

Table 3. Reduced Doppler width $\Delta\lambda_D/\lambda$ [10^{-5}] and line radiance in absolute units [$\text{erg s}^{-1} \text{cm}^{-2} \text{sterad}^{-1}$] of the metallic lines observed in the prominence at the east limb, 23°N on Aug.13, 2011; radiance data are compared with Sotirovski (1965).

ion λ_0 [Å]	Sr II 4215	Ca I 4227	Ti II 4468	Fe II 4549	Ba II 4554	Ti II 4563	Mg II 4571	Na I 5890	Na I 5896
reduced width	2.37	2.31	1.21	1.59	1.15	1.59	(0.87)	1.20	1.14
obs. radiance	116	36.1	31.1	19.1	21.5	21.8	6.7	70	46
Sotirovski	34.3	21.8	7.5	7.3	4.2	4.5	6.3	4.8	4.4

These cool (and dense) prominence cores emit the narrow Na D lines which correspond to low T_{kin} and v_{nth} values as, e.g., the 7000 K and 2.8 km/s for August 13 in Figure 5.

The broad He lines, however, originate in hotter prominence regions where collisional excitation (and ionization) becomes effective. The observed "hierarchy" of excess broadening from He I singlet to He I triplet and He II lines may either be explained by differently hot threads or by a PCTR with outwards increasing temperature (or v_{nth}). But the width excess of He II 4685.7 Å corresponds to 40000 K (*cf.*, end of Section 3) which agrees with the formation temperature for He II lines calculated by Gouttebroze and Labrosse (2009). Hence, a temperature increase through the PCTR, as assumed in the models by Heinzel and Anzer (2001), may be more realistic than an increase of v_{nth} . Also a combined outwards increase of both, T_{kin} and v_{nth} , might fit our observations.

The singly ionized metallic lines show a similar width excess as He I 4471 Å: In Figure 5 their v_0 exceed ≈ 1.2 times the values expected for [$T_{\text{kin}} = 7000 \text{ K}$; $v_{\text{nth}} = 2.8 \text{ km/s}$]. Hence, the singly ionized metallic lines may be emitted from similar layers as the He I triplet line. The rather tight relation of radiance and widths of Na D, He I 4471 Å and He II 4686 Å (see Tables 1 and 2) favors a PCTR surrounding each individual thread rather than the prominence as a whole.

Acknowledgements N. Labrosse kindly put the model means at our disposal. We thank an unknown referee for fruitful comments, J. Hirzberger (MPS) for his code of fine-structure superposition and U. Nolte (GWDG) for the figure layout. The research at IRSOL is financially supported by the Canton Ticino, the foundation Aldo e Cele Daccò, the city of Locarno, the local municipalities, and the SNF grant 200020-127329. R. R. acknowledges the foundation Carlo e Albina Cavargna for financial support.

References

- Engvold, O., Livingston, W.: 1971, High Dispersion Spectroscopic Study of Quiescent Prominences. *Solar Phys.* **20**, 375.
- Gouttebroze, P., Labrosse, N.: 2009, Radiative transfer in cylindrical threads with incident radiation. VI. A hydrogen plus helium system. *Astron. Astrophys.* **503**, 663.
- Heasley, N.J., Mihalas, D., Poland, A.I.: 1974, Theoretical Helium I Emission-Line Intensities for Quiescent Prominences. *Astrophys. J.* **192**, 181.
- Heasley, N.J., Tandberg-Hanssen, E., Wagner, W.J.: 1975, Study of He I emission lines in the solar atmosphere. III - The triplet-singlet line intensity ratios in solar prominences. *Astron. Astrophys.* **40**, 391.
- Heinzel, P., Anzer, U.: 2001, Prominence fine structures in a magnetic equilibrium: Two-dimensional models with multilevel radiative transfer. *Astron. Astrophys.* **375**, 1082.
- Hirayama, T.: 1972, Ionized He in Prominences and Chromosphere. *Solar Phys.* **24**, 310.
- Hirayama, T., Nakagomi, Y.: 1974, Observations of Prominences in He II with a New 25 CM Coronagraph. *Pub. Astron. Soc. Japan* **26**, 53.
- Illing, R.M.E., Landman, D.A., Mickey, D.L.: 1975, Observations of helium and hydrogen emission in quiescent prominences. *Solar Phys.* **45**, 339.
- Jordan, S., Andretta, V., Garcia, A., Falconer, D.: 1997, Understanding the Hell 304 Å Resonance Line in the Sun. In: Wilson, A. (ed.) *Fifth SOHO Workshop: The Corona and Solar Wind Near Minimum Activity* **404**, ESA, Noordwijk 439.
- Labrosse, N., Gouttebroze, P.: 2004, Non-LTE Radiative Transfer in Model Prominences. I. Integrated Intensities of He I Triplet Lines. *Astrophys. J.* **617**, 614.
- Labrosse, N., Heinzel, P., Vial, J.-C., Kucera, T., Parenti, S., Gunár, S., Schmieder, B., Kilper, G.: 2010, Physics of Solar Prominences: I-Spectral Diagnostics and Non-LTE Modelling. *Space Sc. Rev.* **151**, 243.
- Labs, D., Neckel, H.: 1970, Transformation of the absolute solar radiation data into the 'International Practical Temperature Scale of 1968'. *Solar Phys.* **15**, 79.
- Landman, D.A.: 1985, A new property of the small-scale nonthermal motions in quiescent prominences. *Astrophys. J.* **295**, 220.
- Patsourakos, S., Vial, J.-C.: 2002, Soho Contr. to Prominence Science. *Solar Phys.* **208**, 253.

-
- Poletto, R.M. G.: 1967, The spectra of some quiescent prominences observed during the total solar eclipse of 1952, February 25 - Nota I. *Mem. Soc. Astr. Italiana* **38**, 479.
- Ramelli, R., Bianda, M., Stenflo, J.O., Jetzer, P.: 2006, Solar Research Programs at IRSOL, Switzerland. In: Ramelli, R., Shalabiea, O., Saleh, I., Stenflo, J. O. (ed.) *Proc. Intern. Symp. on Solar Phys. and Solar Eclipses, Waw an Namos, Libya, March 2006*, 121.
- Ramelli, R., Balemi, S., Bianda, M., Defilippis, I., Gamma, L., Hagenbuch, S., Rogantini, M., Steiner, P., Stenflo, J.O.: 2010, ZIMPOL-3: a powerful solar polarimeter. In: McLean, I. S., Ramsay, S. K., Takami, H. (ed.) *Proc. Soc. Photo-Opt. Instr. Eng. (SPIE)* **7735**, 66.
- Sotirovski, P.: 1965, Contribution à l'étude de la couronne lors de l'éclipse du 15 février 1961. III. Raies d'émission de la protubérance observée à Hvar. *Ann. d'Astrophys.* **28**, 106.
- Stellmacher, G., Wiehr, E.: 1970, Magnetically Non Split Lines in Sunspots. *Astron. Astrophys.* **7**, 432.
- Stellmacher, G., Wiehr, E.: 1994, The H α and H β emissions in solar prominence structures. *Astron. Astrophys.* **290**, 655.
- Stellmacher, G., Wiehr, E.: 1995, Branching of the helium-to-Balmer emission ratio in solar prominence structures. *Astron. Astrophys.* **299**, 921.
- Stellmacher, G., Wiehr, E.: 1997, The helium singlet-to-triplet line ratio in solar prominences. *Astron. Astrophys.* **319**, 669.
- Stellmacher, G., Wiehr, E.: 2005, Solar prominences with Na and Mg emissions and centrally reversed Balmer lines. *Astron. Astrophys.* **431**, 1069.
- Stellmacher, G., Wiehr, E., Dammasch, I.E.: 2003, Spectroscopy of solar prominences simultaneously from space and ground. *Solar Phys.* **217**, 133.
- Tandberg-Hanssen, E., Zirin, H.: 1959, Physical Conditions in Limb Flares and Active Prominence. I. The Loop Prominence of Nov. 12 and 22, 1956. *Astrophys. J.* **129**, 408.
- Worden, S.P., Beckers, J.M., Hirayama, T.: 1973, The He⁺ λ 4686 line in the low chromosphere. *Solar Phys.* **28**, 27.
- Yakovkin, N.A., Zeldina, M.Y.: 1971, The Helium Radiation in Prominences. *Solar Phys.* **19**, 414.